An Adaptive Multi-Objective Evolutionary Algorithm With Human-Like Reasoning For Enhanced Decision-Making In Building Design

Michael S. Bittermann
Department of Building Technology
Delft University of Technology
Delft, The Netherlands
m.s.bittermann@tudelft.nl

I. Sevil Sariyildiz
Department of Building Technology
Delft University of Technology
Delft, The Netherlands
i.s.sariyildiz@tudelft.nl

Abstract— **An adaptive multi-objective genetic algorithm is presented, where a fuzzy system is used for the fitness evaluation. The adaptivity of the evolutionary algorithm refers to modifying in a measured way the degree of relaxation of the conventional Pareto dominance concept that is used to grade solutions in multi-objective space. The aim of the adaptive relaxation is to retain adequate selection pressure during the search process. The fuzzy system models human-like reasoning that is used to evaluate the suitability of candidate solutions. This way vagueness and imprecision inherent to criteria is taken care of. Next to that, due to the use of fuzzy information processing, the resulting Pareto optimal solutions may be distinguished regarding their suitability for the ultimate goal, although from the Pareto dominance viewpoint the solutions are equivalent. This yields relevant information for a decision maker, so that some of the difficulties to select among the Pareto optimal solutions are alleviated. The algorithm is implemented for a decision making problem from the domain of architecture, where an optimal spatial arrangement of a multi-functional building is sought that satisfies three soft objectives.**

Keywords- evolutionary multi-objective optimization, genetic algorithm, Pareto dominance, fuzzy information processing, cognitive systems

I. INTRODUCTION

In many real-world decision making (dm) tasks several goals are to be satisfied at the same time. Some of the goals may be soft, that is they involve vagueness and imprecision. Examples of such goals are 'high functionality' and 'low cost.' Due to their soft nature, establishing their relative importance in a dm task is difficult to accomplish with certainty, in particular prior to establishing information on the inevitable trade-offs inherent to the task. This entails that the objectives may not be combined into a single criterion, i.e. the dm problem is not to be treated as a single-objective optimization problem. Therefore, multi-objective optimization became an important approach for dm purposes. To deal with the increasing complexity of the multi-objective optimization tasks *direct* search methods that are based on a population of solutions became the dominant approach. The directness of the methods refers that only objective function values are used to drive the search in contrast to the gradient-based methods, where derivative vectors are used for this purpose. The most prominent direct, population-based algorithms are evolutionary algorithms (MOEAs) and particle swarm optimization algorithms (PSO), and these are extensively being investigated for solving associated optimization problems, e.g. [1-5]. Population-based algorithms are particularly suitable for multi-objective optimization, since they evolve simultaneously a population of potential solutions. These solutions are investigated in non-dominated solution space, so that the optimized solutions in a multi-objective functions space form a front which is known as Pareto surface or front. Although Pareto front is an important concept, its formation is not straightforward since the strict search of non-dominated regions in the multi-objective solution space prematurely excludes some of the potential solutions that results in aggregated solutions in this very space. This means the Pareto surface does not fully develop and the diversity of the solutions on the Pareto front is not fully exercised. Conventionally, non-dominated solutions with many objectives are usually high in number, making the selection pressure toward the Pareto front low, with aggregated solutions in the Pareto dominance-based MOEA algorithms [6]. The purpose of this paper is to provide a solution, where convergence together with diversity of solutions on the Pareto front is maintained [7]. This work addresses this issue by employing adaptive relaxation of the dominance concept during the search process, where the relaxation implies precise expansion of the dominated region of the search space. The effectiveness of the adaptive relaxation approach w.r.t. diversity preservation is demonstrated with an application from the domain of architectural design, where decision on optimal spatial configuration satisfying multiple objectives is pursued. In the application human-like reasoning is employed during the fitness evaluation, so that ultimate selection among Pareto solutions by a decision maker is facilitated.

Section two of this paper describes the adaptive relaxation of the Pareto dominance concept. Section three describes an application, where adaptive and conventional Pareto ranking, are compared. This is followed by conclusions.

978-1-61284-069-7/11/$26.00 ©2011 IEEE

II. ADAPTIVE RELAXATION OF PARETO DOMINANCE

In Multi-objective (MO) algorithms that are population-based, such as MOEA or Multi-objective Particle Swarm optimization (MOPSO), in many cases the use of Pareto ranking is a fundamental selection method. Its effectiveness is clearly demonstrated for a moderate number of objectives, which are subject to optimization simultaneously [8]. Pareto ranking refers to a solution surface in a multidimensional solution space formed by multiple criteria representing the objectives. On this surface, the solutions are diverse but they are assumed to be equivalently valid. The driving mechanism of the Pareto-ranking based algorithms is the conflicting nature of criteria, i.e. increased satisfaction of one criterion implies loss with respect to satisfaction of another criterion. Therefore the formation of Pareto front is based on objective functions of the weighted N objectives $f_1, f_2, ..., f_N$ which are of the form

$$F_i(\boldsymbol{x}) = f_i(\boldsymbol{x}) + \sum_{j=1, j\neq i}^{j=N} a_{ji} f_j(\boldsymbol{x}), i = 1, 2, ..., N \qquad (1)$$

where $F_i(x)$ are the new objective functions; a_{ji} is the designated amount of gain in the j-th objective function for a loss of one unit in the i-th objective function. To find the Pareto front of a maximization problem we assume that a solution parameter vector $\boldsymbol{x}_1$ dominates another solution $\boldsymbol{x}_2$ if $F(\boldsymbol{x}_1) \geq F(\boldsymbol{x}_2)$ for all objectives. At the same time a contingent equality is not valid for at least one objective.

In solving multi-objective optimization tasks, with the increase of the number of objective functions, i.e. with high dimensionality, the effectiveness of the Pareto ranking in this strict form is hampered. Namely, with many objectives, there are few solutions that dominate others in the strict dense expressed by (1). This means the search has little information to distinguish among solutions, so that the selection pressure pushing the population into the desirable region is too low. Therefore the algorithm prematurely eliminates potential solutions from the population, exhausting the exploratory potential of the population. As a result the search arrives at an inferior Pareto front with aggregation of solutions along this front. The issue of solution diversity and effective solution for multi-objective optimization problem described above can be understood considering that the conventional Pareto ranking implies a kind of *greedy* algorithm, which considers the solutions at the search area delimited by orthogonal axes of the multidimensional space, i.e. a_{ji} in (1) becomes zero. This is shown in figure 1 by means of the orthogonal lines delimiting the dominated region of the search space. The point P in figure 1 is ultimately subject to identification as an ideal solution, as the figure describes a maximization problem. To increase the pressure pushing the Pareto surface towards to the maximally attainable solution point is the main problem, and relaxation of the orthogonality with a systematic approach is an appealing solution and applied in this work. Although, some relaxation of the dominance is addressed in literature [9, 10], in a multidimensional space to identify the size of relaxation corresponding to a volume is not explicitly determined. In In such a volume next to non-dominated solutions, dominated but potentially favourable solutions, as described above, lie. To determine this volume optimally as to the circumstantial

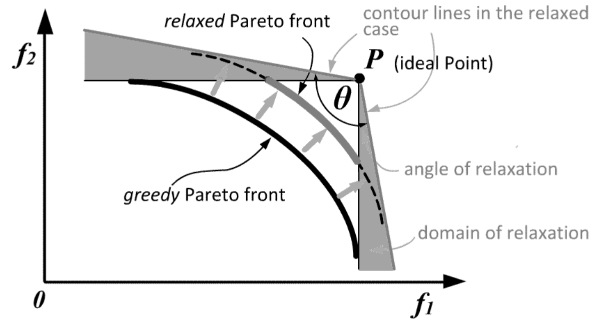

Figure 1. Contour lines defining the dominated region of the search space in relaxed versus 'greedy' Pareto dominance case for a maximization problem.

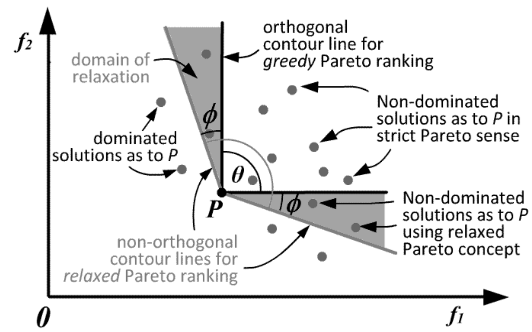

Figure 2. Implementation of the relaxation concept during the evolutionary search process for a maximization problem

conditions of the search process is a major and a challenging task. In this work the solution for this task is due to the mathematical treatment of the problem, where the volume in question is identified adaptively during the search that it yields a measured pressure to the Pareto front towards the desired direction, at each generation as follows.

The fitness of the solutions can be ranked by the fitness function

$$\boldsymbol{R}_{fit} = \frac{1}{N(\phi) + n}, \qquad (2)$$

where n is the number of potential solutions falling into the *search domain* consisting of the conventional orthogonal quadrant, with the added areas of relaxation. N is a function of the relaxation angle, yet before explaining its functionality we consider details of the relaxation. For each solution point, say P in figure 2, the point is temporarily considered to be a reference point as origin, and all the other solution points in the orthogonal coordinate system are converted to the non-orthogonal system coordinates. This is accomplished using the matrix operation given by (3) [11]

$$F = \begin{bmatrix} F_1 \\ F_2 \\ \cdots \\ F_n \end{bmatrix} = \begin{bmatrix} 1 & a_{21} & ..... & a_{n1} \\ a_{12} & 1 & ..... & a_{1n} \\ .... & & & \\ a_{1n} & a_{2n} & ..... & 1 \end{bmatrix} \begin{bmatrix} f_1 \\ f_2 \\ ..... \\ f_n \end{bmatrix} = \begin{bmatrix} 1 & \tan(\phi_2) & ..... & \tan(\phi_n) \\ \tan(\varphi_2) & 1 & ..... & \tan(\varphi_n) \\ .... & & & \\ \tan(\gamma_2) & \tan(\gamma_n) & ..... & 1 \end{bmatrix} \begin{bmatrix} f_1 \\ f_2 \\ ..... \\ f_n \end{bmatrix} \qquad (3)$$

where the angles ϕ, φ, ... γ represent the respective relaxation angles between one axis of the coordinate system and the other axes. After coordinate transformation using (3), all points which have positive coordinates in the non-orthogonal system correspond to potential solutions contributing to the next generation in the evolutionary computation. If any point possesses a negative component in the new coordinate system, the respective solution does not dominate *P* and therefore is not counted. This is because otherwise such a solution may lead the search in a direction away from *P*. The importance of this coordinate transformation becomes significant especially with greater amounts of objective dimensions. It is emphasized that increasing the angle θ in figure 2 by a small angle denoted ϕ in the figure, corresponds to increasing the dominated region of the entire search domain also by ϕ as seen in figure 2.

Determination of the suitable relaxation angle depends on the particular conditions occurring during the stochastic search process. In general a wide average angle is expected to provide more diversity in the population for the next generation. However, when the relaxation angle would be excessively big, the population for the next generation can be crowded with trivial solutions. To prevent that, in (2) the number of non-dominated solutions with respect to the particular solution considered denoted by *n*, is summed up with the function of the angle $N(\theta)$. Adaptively changing the angle in an evolutionary algorithm implies that every chromosome contains its own associated relaxation angle, so that the angle is subject to the usual genetic operations. Therefore the average angle $\bar{\theta}$ of the population is changing for every generation adaptively. When a chromosome has a wider relaxation angle the conditions necessary for it to be non-dominated are stricter compared to a solution with a small angle. To 'balance' this, $N(\theta)$ in (4) represents a number of *virtual solutions* that are accrued to the counted number of dominant solutions denoted by *n* in (2).

$$N(\theta) = \frac{s}{1+\left(\theta/\bar{\theta}\right)} \tag{4}$$

Considering (2) and (4) together it is clear that the purpose is to reward a chromosome for affording a wide relaxation angle θ, relative to the average $\bar{\theta}$ angle associated to the members of the population, and still having a low dominance count denoted by *n*. This means for instance that between two solutions with the same amount of non-dominated solutions, the one with the wider angle is preferred. It is noted that the number *s* appearing in (4) is a constant number, used to adjust the relative significance of relaxation angle versus count *n*. This means the value of *s* should be selected bearing in mind particularly population size, so that solutions using wide angles are adequately rewarded, for instance.

III. Application for Enhanced Decision-Making in Building Design

A. *Problem Description*

A layout problem of a building complex is considered, where the spatial arrangement of a number of spatial units is to be accomplished in such a way that three main goals are satisfied simultaneously. These goals are maximizing the building's functionality and energy performance, as well as its performance regarding form related preferences. The building

Figure 3. Design objects subject to optimal positioning on the building site

subject to design consists of a number of spatial units, referred to as design objects, where every unit is designated to a particular purpose in the building. The task is to locate the objects optimally on the building site with respect to the three objectives forming suitable spatial arrangements. The objects are seen from figure 3.

In order to let the computer generate a building from the components shown in figure 3, i.e. for a solution to be feasible, it is necessary to ensure that all solutions have some basic properties. These are that spaces should not overlap, and objects should be adjacent to the other objects around and above. This is realized in the present application by inserting the objects in a particular sequential manner into the site. This is illustrated in figure 5. Starting from the same location, one by one the objects are moved forward, i.e. translated in northern direction, until they reach an obstacle. An obstacle is either the site boundary or another object previously inserted. When an object touches a previously inserted one, the former object changes its movement direction from the northern to the eastern direction, moving east until again it reaches the site boundary or another object. As a final movement step the inserted object will move downward until it touches the ground plane. Packing objects in two dimensions in this way is known as *bottom-left two heuristic packing routine* in literature, e.g. [12]; yet it is noted that the objectives in conventional packing problems significantly differ from architectural design problems. For instance in the former case the adjacency or nearness of objects is usually irrelevant, whereas in building design it is relevant. The same counts for energy related matter like exposure of facades in north or south directions. Objects exceeding the site boundary will be inserted using a second movement procedure, where, in a similar way as before, the objects are moved onto the buildings already inserted. This is seen from figure 5c and 5d.

In order to deal with the abstract nature of goals involved in the task, a particular kind of knowledge model, namely a fuzzy neural tree, is employed to assess the suitability of a solution based on human-like reasoning. A neural tree is composed of terminal nodes, non-terminal nodes, and weights of connection links between two nodes. The non-terminal nodes represent neural units and the neuron type is an attribute introducing a non-linearity simulating a neuronal activity. In the present case, the non-linearity is established by means of a Gaussian function, which has several desirable features for the intended goals; namely, it is a radial basis function ensuring a solution

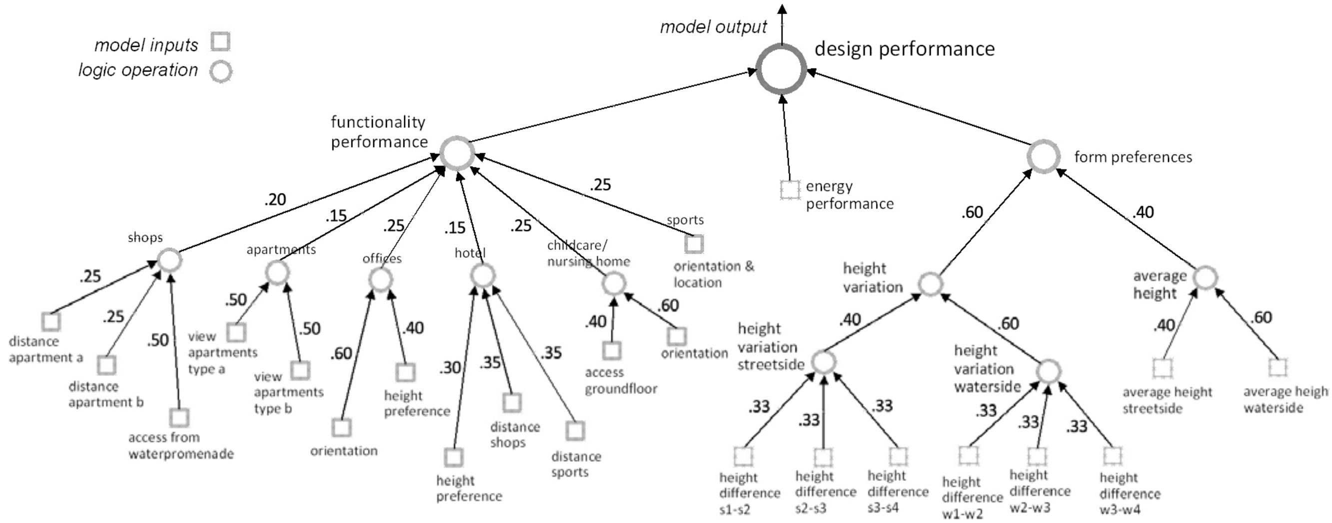

Figure 4. Fuzzy neural tree for performance evaluation of the candidate solutions

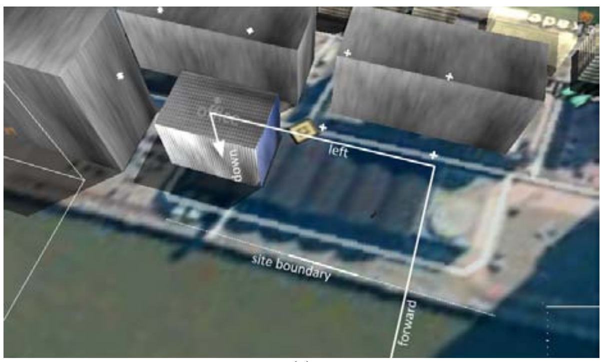

(a)

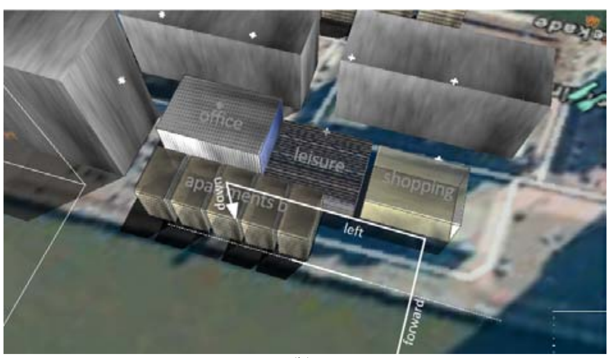

(b)

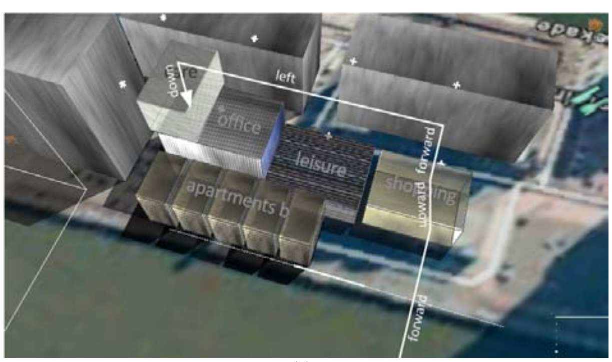

(c)

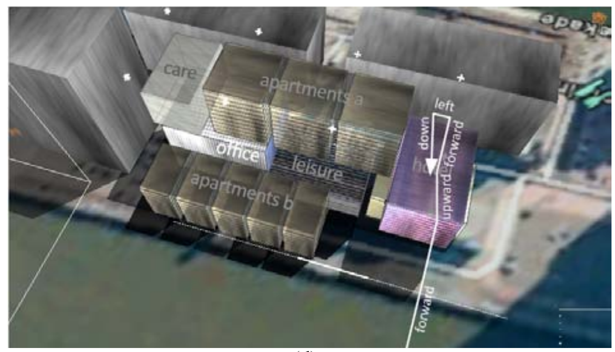

(d)

Figure 5. Generation process of a solution through sequential insertion of the design objects

as well as the smoothness. At the same time it plays the role of a fuzzy membership function in the tree structure, which is considered to be a fuzzy logic system, as its outcome is based on fuzzy logic operations and thereby associated reasoning. The root node of the neural tree shown in figure 4 describes the ultimate goal subject to maximization, namely the design performance and the tree branches form the objectives constituting this goal. The connections among the nodes have a weight associated with them, as seen from the figure. The weights are given by a decision maker, specifying the relative significance a node has for the node one level closer to the root node as an expression of knowledge. The weights and input information is processed at each inner node of the tree model based on a fuzzy AND operation given by [13]

$$O_j = \exp(-\frac{1}{2}\sum_i^n \left[\frac{(\mu_i - 1)}{\sigma_j / w_{ij}}\right]^2) \qquad (5)$$

where O_j is the output of the j-th inner node, μ_i denotes the strength of the i-th input coming to this node; w_{ij} denotes the relative importance of this input; and σ_j a parameter responsible to ensure a consistency in the AND operation,

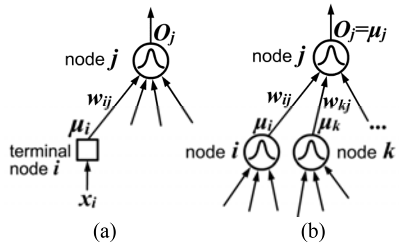

Figure 6. Different type of node connections in the neuro-fuzzy model in figure 4

which needs to be identified before the computations can be carried out. In order to provide the neural model with input values, fuzzification processes are carried out at the terminal nodes shown by means of square shaped boxes in figure 4. The fuzzification yields the degree of satisfaction for the elemental requirements in the form of membership degrees. Two examples of the fuzzification are shown in figure 7.

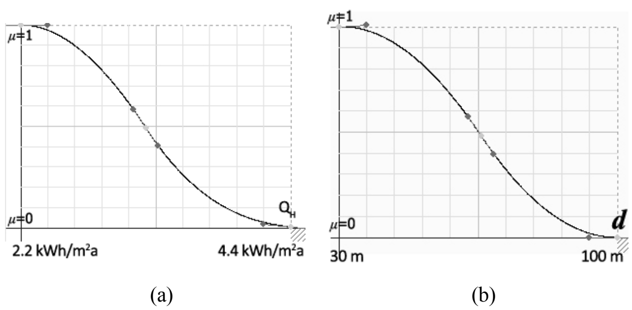

Figure 7. Fuzzy memberhips functions at two of the terminal nodes in figure 4 for energy performance evaluatioon(a); for evaluation of the average building height along the waterfront (b)

For instance concerning the requirements on average height of the building the decision maker prefers to have a low average height along the street side to give the building a less dominant expression when perceived by people walking along the waterfront. This requirement is seen from the membership function in figure 7b, where the membership degree diminishes with increasing height.

The fuzzified information is then processed by the inner nodes of the tree. These nodes perform the AND operations using Gaussian membership functions as described above, where the width-vector of the multi-dimensional Gaussian reflects the relative importance among the inputs to a node. Finally this sequence of logic operations starting from the model input yield the performance at the penultimate node outputs of the model. This means the more satisfied the elemental requirements at the terminal level are, the higher the outputs will be at the nodes above, finally increasing the design performance at the root node of the tree. Next to the evaluation of the design performance score, due to the fuzzy logic operations at the inner nodes of the tree, the performance of any sub-aspect is obtained as well. This is a desirable feature in design decision making, which is referred to as transparency. The neural model is used during the evolutionary search process to evaluate the fitness of solutions, in order to arrive at designs with maximal design performance. In the multi-objective implementation the outputs of the nodes *functionality*, *energy*, and *form preferences*, which are the penultimate nodes, are subject to maximization. Their values are used in the fitness determination procedure of the genetic algorithm. Employing the fuzzy neural tree in this way the genetic search is equipped with some human-like reasoning capabilities during the search. It is noted that due to the use of fuzzy logic in this work, the objective space is a hyper cube having the size of unity along every dimension. Therefore in implementation of (3) the angles of relaxation are taken to be symmetrical w.r.t. the line defined by the origin and the utopic point, i.e. all elements a_{ij} of the matrix in (3) take the same value.

B. Systematic Distinction Among Pareto Optimal Solutions

In complex problems addressed by population-based algorithms, the amount of Pareto optimal solutions a decision maker needs to consider may be high in order to identify an ultimately favorable solution. It is noted that during this process, to retain precision in second-order preferences is necessary, yet problematic to ensure. Therefore it becomes desirable to obtain information about the relative ultimate suitability among the Pareto optimal solutions. Such information is attained due to the involvement of fuzzy modelling in this work, as follows.

From figure 4, at the root node, the performance score is computed by the defuzzification process given by

$$w_1 f_1 + w_2 f_2 + w_3 f_3 = p\,, \qquad (6)$$

where f_1 is the output of the node *functionality performance;* f_2 of node *energy performance*; f_3 of node *form preferences.* That is, they denote the performance values for these aspects of the design, which are subject to simultaneous maximization. The variable p denotes the design performance which is also requested to be maximized, which is the ultimate goal of the design. In (6) w_1, w_2 , and w_3 denote the weights associated to the connections from f_1, f_2 and f_3 to the design performance. It is noted that $w_1+w_2+w_3=1$. In many real-world decision making tasks the cognitive viewpoint plays an important role. This means it is initially uncertain what values $w_1,\ldots w_3$ should have. Namely, the node outputs $f_1, \ldots, f_3$ can be considered as the *design feature vector,* and the reflection of these features can be best performed if the weights w_1 ; …; w_3 define the same direction as that of the feature vector. This implies that the performance p_{max} for each genetic solution is given by [13].

$$p_{\max} = \frac{f_1^2 + f_2^2 + f_3^2}{f_1 + f_2 + f_3}\,, \qquad (7)$$

Therefore, p_{max} in (7) is computed for all the design solutions on the Pareto front. Then the *solution with maximal p_{max} performance* is selected among the Pareto solutions. This way the particular design is identified as a solution candidate with the corresponding $w_1, w_2, \ldots, w_n$ weights. These weights form a priority vector $\boldsymbol{w^*}$. If for any reason this candidate solution is not appealing, the next candidate is searched among the available design solutions with a desired design feature vector and the relational attributes, i.e., $w_1, w_2, \ldots, w_n$. One should note that, although performance does not play role in the genetic optimization, Pareto front offers a number of design options with fair performance leaving the final decision dependent on other environmental preferences. Using (7), second-order preferences are identified that are most promising for the decision making task at hand, where ultimately maximal solution performance is pursued. To make the analysis explicit we consider a two-dimensional objective space. In this case, (7) becomes [11]

$$p = \frac{f_1^2 + f_2^2}{f_1 + f_2}, \quad (8)$$

which can be put into the form

$$f_1^2 + f_2^2 - pf_1 + pf_2 = 0 \quad (9)$$

that defines a circle along which the performance is constant. To obtain the circle parameters in terms of performance, we write

$$f_1^2 + f_2^2 - pf_1 + pf_2 \equiv (x - x_1)^2 + (y - y_1)^2 - R^2 \quad (10)$$

The performance circle with the presence of a Pareto front is schematically shown in figure 8. From the figure, it is seen that the maximum performance is at locations, where one of the objectives is maximal at the Pareto front. If both objectives are equal, the maximal performance takes a lower value. This result is significant, since it reveals that in the particular design task with an associated Pareto front shown in figure 8a, a design has a better performance in an unbiased sense if some measured extremity in one way or other is exercised. It is meant that, if a better performance is obtained, then most presumably some extremity will be observed in this design in the sense that one objective is taken relatively much more significant than the others. It is noted that the location of an expected superior Pareto optimal solution in this unbiased sense depends on the shape of the Pareto front, in particular on the degree of symmetry the Pareto front has w.r.t. the line passing from the origin of the objective space through the utopic point. This is seen from figure 8a, where, due to a Pareto front that is asymmetrical w.r.t. to this diagonal, a unique location of a solution with a superior performance may exist. In case of symmetry to the diagonal two areas of superior optimal solutions may exist. This is seen from figure 8b.

C. *Application Results*

In order to investigate the effect of the adaptive relaxation with respect to solution diversity and performance of solutions, the adaptive algorithm is executed and compared against the conventional Pareto ranking. In the adaptive execution s=16 in (4) is taken.

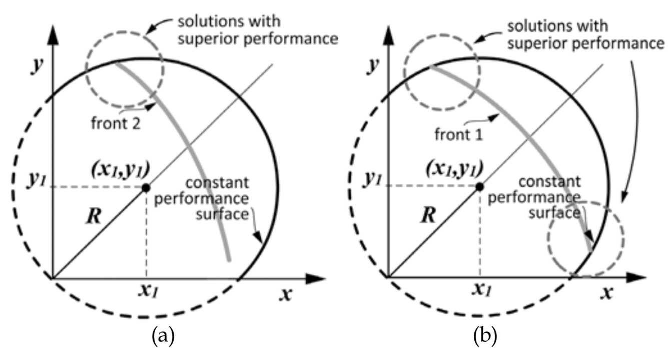

Figure 8. Dependence of the location of desirable solutions on the shape of Pareto front: front that is assymmetrical to the line passing from origine to the utopic point (a); symmetrical front (b)

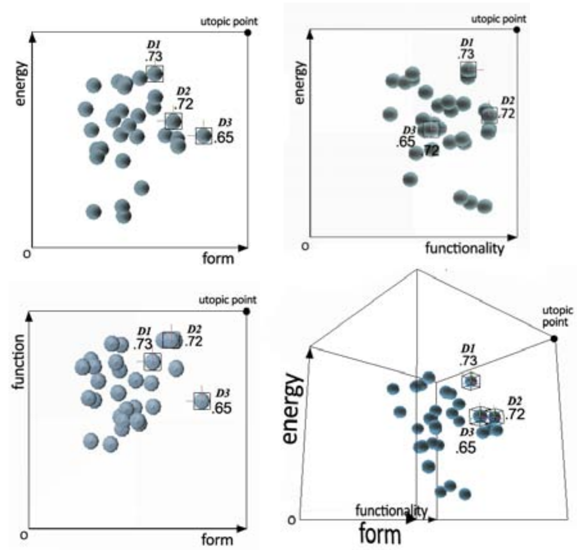

Figure 9. Pareto front after 15 generations using adaptive relaxed Pareto ranking during the search process, where s=16

It is noted that both executions start from the same initial random population. The resulting Pareto front after 15 generations is shown in figures 9 and 10 for the respective cases. The numbers in the figures express the p_{max} value for the respective solution, obtained using (7). Comparing figure 9 and figure 10 it is seen that the adaptive relaxed Pareto ranking yields a more compact shape of the front with solutions at similar sized, small intervals, while in the greedy case the front is more spread out in the objective space, and more scattered. That is in the latter case there are large gaps between solutions, and also there are a number of areas, where a number of solutions are crowding. This is explained from figure 1: Due to the modified solution space in the relaxed Pareto ranking case the Pareto front is able to arise more close to the Utopic Point. Since solutions outside the orthogonal space in figure 1 do not exist, a higher density of population members is expected along the Pareto front compared to the greedy case.

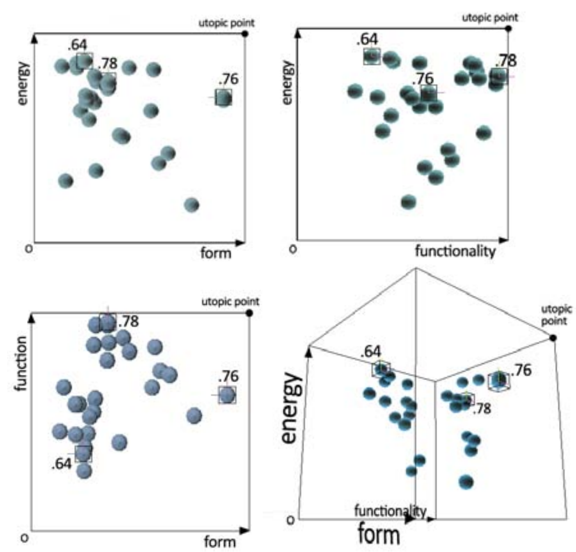

Figure 10. Pareto front after 15 generations using conventional 'greedy' Pareto ranking during the search process

On the other hand it is noted that the conventional algorithm produces individual solutions with higher maximal performance compared to the adaptive case, which is an advantage of the greedy approach when an individual high performance solution is sought, and freedom in decision making as to second order preferences would not be required.

In order to compare the degree of aggregation, the average density among solutions is considered. As a measure of density the average Euclidian distance d between a chromosome and the two chromosomes nearest to it in Euclidian sense, is computed as given by

$$\bar{d} = \frac{\sum_{c=1}^{r}\left[\left(\sum_{i=1}^{n}\sqrt{\left(p_{c,i}-q'_{c,i}\right)^2}+\sum_{i=1}^{n}\sqrt{\left(p_{c,i}-q''_{c,i}\right)^2}\right)/2\right]}{r} \quad (11)$$

where $p_{c,i}$ is the objective function value of chromosome c in the i-th objective dimension, and $q'_{c,i}$ is the objective function value in the same dimension of the chromosome nearest to c, and $q''_{c,i}$ denotes this quantity for the second nearest chromosome. The value r denotes the population size. It is noted that due to the fuzzy modeling emplyed in this work, the maximum value for $p_{c,i}$ and $q_{c,i}$ is unity and their minimum value is zero. A low value for d in (12) indicates that solutions are aggregated; conversely, a high value for d indicates diversity among the solutions in objective space. The result from the adaptive case compared to the greedy case is seen from figure 11.

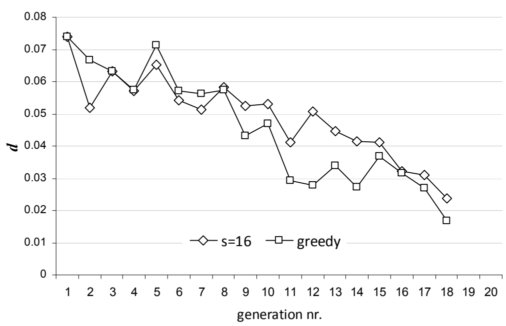

Figure 11. Average distance d in (4) in adaptive relaxed case, where s=16, compared to the 'greedy' case of conventional Pareto ranking

From the figure it is seen that during the early stage of the search process the diversity of the greedy process is occasionally higher compared to the adaptive case. This is explained from the fact that it requires a number of generations until the adaptive d diminishes after 9 generations, i.e. aggregation starts to occur. In contrast to this, the adaptive search with s=16 retains the diversity for another five generations before diversity starts to drop. It is also noted that in the adaptive case the aggregation increases gradually and more smoothly compared to the greedy case. In particular the range of the process in generation 10 to 15 reveals the different nature of the conventional ranking compared to the adaptive case. Namely the greediness of the conventional ranking scheme exhausts the diversity of the population, i.e. a few strictly non-dominated solutions start to 'pull' many solutions to their position, and this leads to the aggregated and scattered front seen in figure 10.

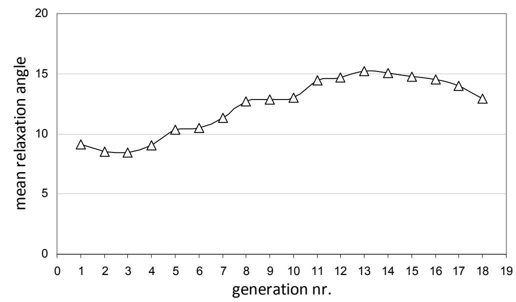

Figure 12. Average relaxation angle throughout the generations

In order to observe the adaptation behavior of the algorithm w.r.t. the relaxation angle, the variation of the average angle throughout the search process is shown in figure 12. From the figure it is seen that the average angle steadily rises to a maximum of 15 degrees in generation 13, and then slightly diminishes again. It is noted that the swiftness of adaptation is determined by the value of s, where a lower value of s ensures quicker adaptation, and vice versa. To understand this let us consider for a non-dominated solution having a large associated angle, say for instance 1.5 times the size of the mean angle. In case s=16 a number of virtual solutions are accrued to the actually counted n number of solutions, namely 6.4 in this case. For smaller values of s the number of accrued virtual solutions is proportionally less. Therefore for larger values of s, good solutions, i.e. solutions having low number of n as well as a large relaxation angle, will relatively less clearly stand out from the other population members, so that they do not so strongly attract other solutions via the genetic operations.

This entails the value for s should be carefully selected, and bearing especially population size in mind, in order to balance the algorithm's exploration versus exploitation behavior [14]. Clearly, greater values of s favor exploration, whereas smaller values of s favor exploitation. In particular the exploration is in the sense that a more refined consideration about the potential of a solution is exercised, namely a seemingly good solution in the sense of a low amount of solutions dominating it, may turn out to be relatively less potent when solutions exist in areas near to the contour lines separating the dominated and non-dominated regions. This information is commonly not used during evolutionary search and it turns out to have merits in particular as to diversity as seen from the comparison above. In this respect it is noted that the algorithm used in this work does not involve means to explicitly 'punish' chromosomes for being in crowded areas of the objective space, as it is often exercised [5]. This is done, so that exclusively the effect of the adaptive relaxation can be observed. It is noted that relaxation of the Pareto concept addresses the root cause of the aggregation phenomenon, rather than addressing exclusively its symptom by reducing fitness of solutions for high crowdedness. For increased effectiveness, combination of relaxed adaptive Pareto ranking and crowding measures are an interesting relevance.

To exemplify the solutions on the Pareto front in figure 9, three resulting Pareto-optimal designs are shown in figure 13. Figure 13a shows design *D1*, 13b shows D2, and 13c shows D3. From figure 9 it is seen that Design *D1*

(a)

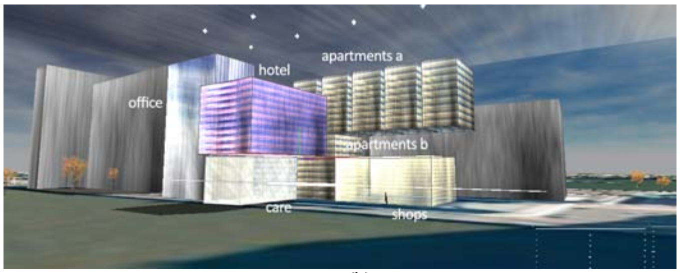

(b)

(c)

Figure 13. Pareto optimal designs, D1 (a); D2 (b); and D3 (c) from figure 9

has the following performance features: functionality .74; energy .75; form .57; p_{max} .73; Design D2 has: functionality .86; energy .58; form .65; and p_{max} .72. Design D3 has: functionality .58; energy .51; form .80; and p_{max} .65. From the results we note that design *D1* outperforms the other two designs as to its p_{max} value, despite the fact that the other two designs perform better on the form aspect. This is explained from the fact that the Pareto front in the present decision making task is not symmetrical to the diagonal line in objective space, as illustrated schematically in figure 8a. The front obtained is oriented in such a way that the form performance is generally lower compared to energy and functionality performance. This means that in the present task, in absence of a-priori second-order preferences, one should not consider form as important as energy and functionality. Considering that D1 and D2 are quite similar as to their maximal performance it is noted that solutions with either outstanding functionality performance, or solutions that perform well on energy and functionality at the same time, are worth to consider in the decision making. However it is noted that many Pareto optimal solutions are not significant from an unbiased viewpoint, that is their p_{max} value is inferior, e.g. in the case of D3. This information is uniquely obtained in this approach, in particular due to the use of fuzzy modeling. It reduces the amount of solutions to consider in the selection among the Pareto solutions and thereby alleviates the decision making task.

IV. Conclusions

An adaptive relaxation approach for enhanced formation of the Pareto front in multi-objective optimization is presented and demonstrated using a decision making task from the domain of architecture. The approach is to adaptively relax the Pareto dominance concept during the search process. The adaptation is found to be favorable for diversity compared to the conventional Pareto ranking, yielding a more compact and less scattered front in the former case. This is seen from the decision making application, where a building consisting of several volumes is obtained, so that three soft objectives pertaining to the building are satisfied. The satisfaction degree is measured using a fuzzy model, so that the evolutionary algorithm makes use of some human-like reasoning during its search. The use of fuzzy information processing entails that a decision maker obtains new information regarding the relative suitability of solutions from an unbiased viewpoint. For example from the application it is seen that *form* related performance plays a less significant role compared to *energy* and *functionality* concerns. This information is relevant in the selection among the Pareto optimal solutions, and it is challenging to be obtained otherwise. As the approach is able to deal with soft issues in decision making, it is deemed suitable for many real world applications having such features.

References

[1] E. Zitzler and L. Thiele, "Multiobjective evolutionary algorithms: A comparative case study and the strength Pareto approach," *IEEE Trans. Evolutionary Computation,* vol. 3, pp. 257-271, 1999.

[2] X. Yao, Y. Liu, and G. M. Lin, "Evolutionary programming made faster," *IEEE Trans. Evolutionary Computation,* vol. 3, pp. 82-102, 1999.

[3] A. E. Eiben, R. Hinterding, and Z. Michaelwicz, "Parameter Control in Evolutionary Algorithms," *IEEE Trans. Evolutionary Computation,* vol. 3, pp. 124-141, 1999.

[4] A. P. Engelbrecht, *Computational Swarm Intelligence*. Chichester, GB: Wiley, 2005.

[5] K. Deb, *Multiobjective Optimization using Evolutionary Algorithms*: John Wiley & Sons, 2001.

[6] H. Sato, H.E. Aguirre, and K. Tanaka, "Controlling Dominance Area of Solutions and Its Impact on the Performance of MOEAs," pp. 5-20, 2007.

[7] M. Laumanns, L. Thiele, K. Deb, and E. Zitzler, "Combining convergence and diversity in evolutionary multiobjective optimization " *Evolutionary Computation,* vol. 10, pp. 262-282, 2002.

[8] C. A. C. Coello, D. A. Veldhuizen, and G. B. Lamont, *Evolutionary Algorithms for Solving Multiobjective Problems*. Boston: Kluwer Academic Publishers, 2003.

[9] J. Branke, T. Kaussler, and H. Schmeck, "Guiding multi-objective evolutionary algorithms towards interesting regions," AIFB University of Karlsruhe, Germany 2000.

[10] K. Deb, J. Sundar, U. Bhaskara, and S. Chaudhuri, "Reference point based multi-objective optimization using evolutionary algorithm," *Int. J. Comp. Intelligence Research,* vol. 2, pp. 273-286, 2006.

[11] Ö. Ciftcioglu and M. S. Bittermann, "Adaptive formation of Pareto front in evolutionary multi-objective optimization," in *Evolutionary Computation*, W. P. d. Santos, Ed. Vienna: In-Tech, 2009, pp. 417-444.

[12] E. Hopper and B. C. H. Turton, "An empirical investigation of metaheuristic and heuristic algorithms for a 2D packing problem," *Eur. J. Oper. Res.,* vol. 128, pp. 34-57, 2001.

[13] M. S. Bittermann and O. Ciftcioglu, "A cognitive system based on fuzzy information processing and multi-objective evolutionary algorithm," in IEEE Conference on Evolutionary Computation - CEC 2009 Trondheim, Norway: IEEE, 2009.

[14] D. E. Goldberg, Genetic Algorithms. Reading, Massachusetts: Addison Wesley, 1989.